Observation of Near-Infrared Dicke Superradiance on Cascading Transitions in Atomic Sodium

M. Gross, C. Fabre, P. Pillet, and S. Haroche
Laboratoire de Spectroscopie Hertzienne de l'Ecole Normale Supérieure, Associé au Centre National de la Recherche Scientifique, 75231 Paris Cedex 05, France

(Received 29 December 1975)

We report the observation of near-infrared Dicke superradiant pulses. The active medium (atomic Na vapor) is optically pumped in the $5S_{1/2}$ state and superradiates on transitions cascading down from this level at 3.41, 2.21, and 9.10 μm. The superradiant character of the emission is checked by studying variations of pulse heights and delays versus initial population inversion density.

Collective spontaneous emission (Dicke superradiance)[1] has been up to now difficult to observe in the optical domain. To our knowledge, the only experiment so far has been performed in the far infrared (100-μm range) on rotational transitions of the HF molecule.[2] In the visible or near infrared, and for Doppler-broadened media, superradiance takes place on a nanosecond time scale, much shorter than the microsecond scale of far-infrared experiments. As a consequence, observation of the phenomenon has been impeded in the past by the lack of very fast and efficient excitation procedures able to prepare within a nanosecond a total population inversion on an optical transition. Using short-pulsed tunable dye lasers, we have optically pumped sodium vapor in the $5S_{1/2}$ state and have observed on transitions cascading down from this level what we believe to be the first direct evidence of Dicke superradiance in the near infrared.

Before describing our observations, let us first recall the main features of superradiance in a pencil-shaped sample having a length L large compared to the wavelength λ of the emitted radiation.[2-4] Let us consider that the atomic population is initially totally inverted on an optical transition a-b (transition probability γ_{ab}). Because of spontaneous emission atoms start falling down from level a to b, each atom developing a randomly phased optical dipole. At low excited-atom density n, these dipoles remain independent of each other and the sample radiates an isotropic fluorescence signal proportional to n with a decay time γ_{ab}^{-1} (usual spontaneous emission). On the other hand, for n large enough, the dipoles of different atoms start interacting with each other through their common coupling with the axial modes of the radiation field, the characteristic coupling time being[2,4] $\tau_R = 8\pi(\gamma_{ab} n L \lambda^2)^{-1}$. After a delay τ_D proportional to τ_R, all the dipoles strongly lock in phase with each other and radiate, along the axis of the active medium, a light pulse with an intensity proportional to n^2. The phenomenon is observable only if τ_R is shorter than the dephasing time T_2^* of the atomic dipoles,[2,4] which sets up the threshold condition for superradiance $n > 8\pi(\gamma_{ab} T_2^* L \lambda^2)^{-1}$. In the optical range, the dominating dephasing process is generally the Doppler effect and T_2^* falls in the nanosecond time scale. It should be noted that the delay time τ_D of the superradiant emission exceeds τ_R and T_2^* and can be of the order of a few tens of τ_R.[2] Let us now particularize this discussion to the Na experiment: Atoms are prepared in the $5S_{1/2}$ level by stepwise excitation from the ground state via the intermediate $3P_{3/2}$ level [see Fig. 1(a)]. All the transitions cascading down from the $5S_{1/2}$ level (except those leading to the ground and the $3P_{3/2}$ states) are totally inverted at a given stage of the atomic decay and may thus exhibit superradiance. These transitions are listed in Table I

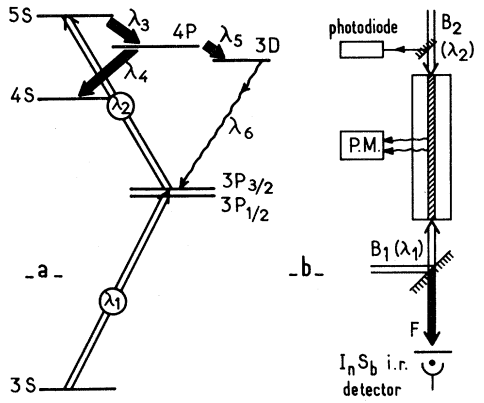

FIG. 1. (a) Diagram of Na energy levels relevant for superradiance experiment. Double-line arrows, pumping transition at $\lambda_1 = 0.5890$ and $\lambda_2 = 0.6160$ μm; solid-line arrows, superradiant transitions $\lambda_3 = 3.41$, $\lambda_4 = 2.21$, and $\lambda_5 = 9.10$ μm; wavy line, transition at $\lambda_6 = 0.8191$ μm detected off-axis by the photomultiplier. (b) Sketch of experimental setup showing collinear pumping beams B_1 and B_2, on-axis InSb detector, and off-axis photomultiplier.

TABLE I. Transitions cascading down from the $5S_{1/2}$ level with their relevant parameters for superradiance.

Transition	λ (μm)	T_2^* (nsec)	$n\tau_R$ (sec cm^{-3})	n_t (cm^{-3})
$5S$-$4P_{3/2}$	3.41	1.7	4	3×10^9
$5S$-$4P_{1/2}$			8	5×10^9
$4P$-$4S$	2.21	1.1	5	5×10^9
$4P$-$3D_{5/2}$	9.10	4.6	23	5×10^9
$4P$-$3D_{3/2}$			34	7×10^9
$4S$-$3P_{1/2}$	1.14	0.6	16	3×10^{10}
$3D$-$3P_{1/2}$	0.82	0.4	16	4×10^{10}
$5S$-$3P_{1/2}$	0.615	0.3	200	6×10^{11}

with the relevant parameters T_2^*, $n\tau_R$, and the threshold density, $n_t = n\tau_R/T_2^*$ for superradiance.[5] In a pressure range corresponding to $n = 10^9$–10^{10} cm^{-3} the three transitions at 3.41, 2.21, and 9.10 μm which are drawn as solid-line arrows in Fig. 1(a) appear to be above threshold. As a result, the system is expected first to go superradiant on the $5S$-$4P$ transition and then, after population has been transferred to the $4P$ levels, to superradiate again on one—or both—of the two competing $4P$-$4S$ and $4P$-$3D$ transitions. If the pressure increases by an order of magnitude ($n \sim 4\times10^{10}$ cm^{-3}) the 1.14- and 0.82-μm transitions should also become superradiant. As for the $5S$-$3P_{1/2}$ transition at 0.615 μm, it has, because of its short wavelength, a very high threshold and is never expected to superradiate since its population inversion is always quenched by the much faster, competing superradiant process at 3.41 μm.

The setup used to detect the superradiant emissions is sketched in Fig. 1(b). Excitation is provided by two optical pulses B_1 and B_2 at $\lambda_1 = 0.5890$ μm ($3S$-$3P_{3/2}$) and $\lambda_2 = 0.6160$ μm ($3P_{3/2}$-$5S_{1/2}$) [see Fig. 1(a)]. These pulses, produced by two dye lasers simultaneously pumped by a 1-MW N_2 laser, are of about 10 kW peak power. They can saturate both λ_1 and λ_2 transitions so that about one quarter of the total number of atoms in the active volume can be prepared in the $5S_{1/2}$ state. The pumping pulses have a duration T_e of about 2 nsec and a spectral width of about 10 GHz, large enough to excite the whole Doppler profiles of the pumping transitions. The pulses propagate along the same axis in order to prepare a pencil-shaped active volume in the 14-cm-long, temperature-regulated, Pyrex cylindrical cell containing Na vapor. A semireflecting mirror allows the separation of the exciting pulses from the superradiant ones emitted along the same axis. A

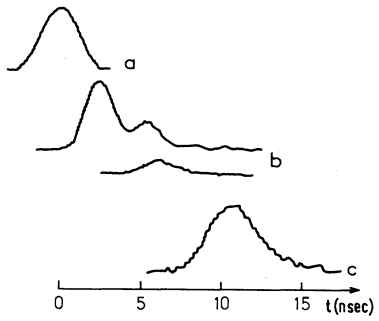

FIG. 2. Time variation of pulse signals monitored by InSb detector. Trace a, exciting pulse B_2; trace b, 3.41-μm pulse for two different excitation intensities; trace c, 2.21-μm pulse for the same excitation as the second 3.41 μm pulse of trace b.

fast infrared InSb detector monitors the infrared signals whose wavelengths are selected by adequate filters F. Furthermore, a photomultiplier detects the fluorescent light emitted off-axis on the $3D$-$3P$ transition at 0.82 μm and thus monitors the population of the $3D$ state. A dual-trace, fast-transient recorder (Tektronix R 7912) analyzes the time variations of the signals. This recorder is triggered by the signal from a photodiode receiving part of the B_2 light beam. This trigger provides, after correction for propagation, the time origin for each sequence of pulses. Using this setup, we have made the following observations:

(a) Above a threshold $n_0 \approx 6\times10^9$ cm^{-3} (Na pressure, 10^{-6} Torr), we have detected in the output of the InSb detector two pulsed, few-nanosecond-long, directively emitted infrared signals whose wavelengths determined by a grating monochromator are 3.41 and 2.21 μm. The 3.41-μm pulse follows laser excitation with a few-nanosecond delay (longest observed delay, 7 nsec). The 2.21-μm pulse is delayed by several nanoseconds with respect to the 3.41 μm one. Figure 2 shows recordings of 3.41-μm pulses (trace b) and a 2.21-μm pulse (trace c) which appear clearly delayed with respect to the exciting pulse B_2 (trace a). The 3.41-μm pulse has been recorded for two different excitation densities to show variations of pulse heights and delays versus excitation (see below). Note also the ringings in the wings of the largest 3.41-μm pulse. Similar ringing has been observed in the far-infrared superradiance experiment.[2] For a given Na pressure above threshold and for a nonsaturating light excitation, the height h and delay τ_D of the pulses are a function of the intensity I of the exciting pulse B_2, varia-

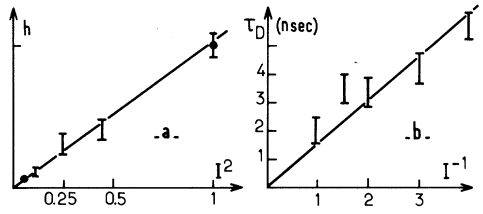

FIG. 3. (a) Height h of 3.41-μm pulse versus I^2, square of B_2 pumping beam intensity. (b) Delay of 3.41-μm pulse versus I^{-1} (I in arbitrary units).

tions of h and τ_D versus I just reflecting the variations of these quantities versus n. In Fig. 3, we have plotted the 3.41-μm pulse amplitude h versus I^2 [Fig. 3(a)] and the delay τ_D after excitation versus I^{-1} [Fig. 3(b)]. Note that in a range of excitation densities $n_0 < n < 4n_0$, the signal increases as n^2 and is delayed as n^{-1}, which is good evidence of its superradiant character. When n is increased above $4n_0$ [$I > 1$ in the arbitrary units of Fig. 3(b)], the delay of the pulse becomes so short that it falls in the wings of the exciting pulse ($\tau_D < T_e \sim 2$ nsec). Consequently, the system starts operating under quasi-stationary conditions, the upper level $5S_{1/2}$ being continuously replenished as the superradiant pulse evolves. The phase correlations between the dipoles of different atoms are then washed out by the regenerative pumping, so that the pulse amplitude is no longer proportional to n^2, but saturates as n. The system is then no longer in a "Dicke superradiant regime" but evolves continuously as n is increased towards a "superradiant laser regime" analogous to the one observed in a high-gain amplifying medium[6] (mirrorless laser).

(b) Above a threshold of about $4n_0$ (4×10^{-6} Torr) when the 3.41- and 2.21-μm pulses are not delayed any longer, we have observed in the photomultiplier current a very sharp burst of fluorescence at 0.82 μm typically delayed by several tens of a nanosecond with respect to the pumping excitation. This burst, represented for increasing excitation intensities in Fig. 4, is obviously due to a delayed and very fast transfer of population from the $4P$ to the $3D$ level and is hence an indirect evidence of a third superradiant emission at 9.10 μm, which cannot be directly detected since the corresponding pulse is absorbed in the Pyrex walls of the cell. Note that the delay corresponding to the maximum of the burst decreases as excitation increases.

(c) Increasing the pressure above 4×10^{-5} Torr ($n > 40n_0$), we have observed, again with the InSb

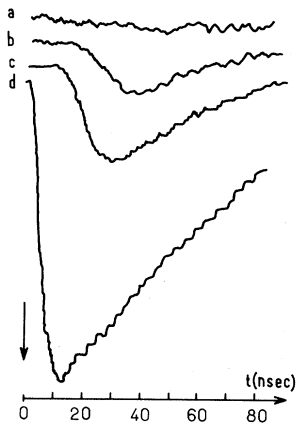

FIG. 4. Time variation of fluorescence signal at 0.82 μm detected by off-axis photomultiplier. Traces a to d correspond to increasing pumping beam intensities at a given Na pressure. Arrow indicates pumping time.

detector, two directively emitted infrared pulses at 1.14 and 0.82 μm, corresponding to the $4S$-$3P$ and $3D$-$3P$ transitions. These pulses occurred however in the wings of the exciting pulse itself and no clear evidence of *delayed* superradiance emission has been obtained at these wavelengths. Difficulties in observing Dicke superradiance on these transitions is obviously linked to their large Doppler effect, yielding very small T_2^* values (see Table I).

A quantitative description of the cascading superradiance effects observed in our experiment, taking into account multilevel operation, inhomogeneous broadening, and propagation effects, remains to be done. The observed competition between the $4P$-$4S$ and $4P$-$3D$ transitions can however be qualitatively understood by the following arguments: Just above threshold, which is nearly the same for both $4P$-$3D$ and $4P$-$4S$ transitions ($n_0 \sim 6\times10^9$), superradiance only occurs on the 2.21-μm transition because the 2.21-μm pulse which has a much shorter τ_R depletes the common upper level $4P$ population before superadiance can build up on the $4P$-$3D$ transition. On the other hand, well above threshold ($n > 4n_0$), the system is no longer in a Dicke superradiant regime on the 2.21-μm transition, but rather, as explained above, in a "quasi-stationary regime." Superradiance at 2.21 μm is then counteracted by pumping and pulse reabsorption in the medium, so that atoms do not fall down any longer to the lower state of the $5S$-$4P$-$4S$ cascade but rather evolve towards a population equilibrium between these states. As a result a large population in-

version is left in the medium on the $4P$-$3D$ transition. This explains that the system can now superradiate after a longer delay at 9.10 μm.

The superradiant effects described in this Letter can have interesting applications. They should be quite generally observed in Rydberg levels which are very close to each other and should easily superradiate on infrared or microwave transitions having a small Doppler effect and hence a very low threshold for superradiance. Extension of our experiments to the visible is also very promising. The major drawback in this case would be the large Doppler effect at short wavelengths. This effect could be reduced by narrowing the width of the pumping dye lasers in order to select a narrow velocity group in the Doppler profile of the pumping transition.

[1]R. H. Dicke, Phys. Rev. 93, 99 (1954).

[2]N. Skribanowitz, I. P. Herman, J. C. MacGillivray, and M. S. Feld, Phys. Rev. Lett. 30, 309 (1973), and in *Laser Spectroscopy*, edited by R. G. Brewer and A. Mooradian (Plenum, New York, 1975).

[3]N. E. Rehler and J. H. Eberly, Phys. Rev. A 3, 1735 (1971).

[4]R. Bonifacio and L. A. Lugiato, Phys. Rev. A 11, 1507 (1975), and references therein.

[5]For calculation of T_2^* in Table I, we apply the formula $T_2^* = 3/\Delta\omega_D$, where $\Delta\omega_D$ is the full Doppler width at half-maximum. For determination of τ_R values, we assume $L = 14$ cm and we use transition rates γ_{ab} given in E. Anderson and V. A. Zilitis, Opt. Spectrosk. 16, 177 (1964) [Opt. Spectrosc. 16, 99 (1964)].

[6]Infrared pulse generation on the $6S$-$5P$-$5S$-$4P$ cascade in potassium excited by a double-quantum process analogous to the one described in this paper has been observed ten years ago [S. Yatsiv, W. G. Wagner, G. S. Picus, and J. F. McClung, Phys. Rev. Lett. 15, 614 (1965)]. This experiment was however performed at a very high K pressure ($n_0 \sim 10^{15}$) so that the system was certainly not Dicke superradiant and operated most likely in a quasi-stationary regime ($\tau_D \ll T_e$).

Observation of Collisionless Heating and Thermalization of Ions in a Theta Pinch*

R. J. Commisso† and Hans R. Griem

Department of Physics and Astronomy, University of Maryland, College Park, Maryland 20742

(Received 25 February 1976)

Spectral line profiles from impurity ions in a small theta pinch have been measured and are interpreted as ion-velocity distribution functions. For antiparallel driving and bias fields, the ions attain a Maxwellian distribution corresponding to a perpendicular temperature of 3–4 keV in a time short compared to particle self-collision times. Thermalization is less rapid for parallel magnetic fields.

Achievement of deuterium and tritium ion temperatures over ~ 5 keV is critical for thermonuclear fusion.[1] In a theta-pinch, imploding electrons and ions acquire the same velocity, because of charge-separation effects.[2] This provides an efficient mechanism for putting directed kinetic energy into ions. In addition, for fusion reactions of the thermonuclear type to occur, the directed ion energy must be randomized.

We measured Doppler-broadened profiles of spectral lines from various oxygen and carbon ions which are natural contaminants and which radiate at different times due to transient ionization. These time-resolved profiles may be interpreted as the (unnormalized) ion velocity distributions. The experiment was performed on a small, 17-cm-diam, 15-kJ theta-pinch device,[3] with peak driving magnetic field $B_z \simeq 17$ kG and quarter period 2.25 μsec. The pinch produced a plasma from an 11-mTorr filling pressure of H_2, and the plasma was diagnosed using magnetic probes and Thomson scattering.[2] Peak electron (proton) temperatures and densities were ~ 250 eV (~ 900 eV) and ~ 6×10^{15} cm^{-3}, respectively.

A 0.5-m monochromator was used to scan the spectral line profiles on a shot-to-shot basis. The instrument function was nearly Gaussian with an instrumental width of 0.53 Å, always much less than the measured widths. Measurements were made both side-on (perpendicular to B_z) and end-on (parallel to B_z). Side-on, the monochromator viewed a 1-cm-high region of the midplane of the coil, centered on the coil axis; end-on, a 3-cm region. In most cases the total line intensity was monitored independently and used to normalize the data. The profiles were obtained for times between 0.61–1.5 μsec after the main bank discharged, i.e., after the implo-